Journal of Optoelectronic and Biomedical Materials Vol. 15, No. 1, January – March 2023, p. 43 -54

# Preparation and mechanical characterization of (rubber blend - micro lead) rubbery composites for shielding application

M. H. Naeem[a,*] , S. H. Hadi Al-Nesrawy[a], M. H. Al-Maamori[b]

[a]*Department of Physics, College of Education for Pure Sciences, University of Babylon, Iraq*

[b]*Department of Polymer and Petrochemical Industries, College of Engineering Materials, University of Babylon, Iraq*

This present work, includes the preparation of rubber batches containing silicone rubber (SIR) (80pphr) and polyurethane (PU) (20pphr) with micro-lead powder in different loading, respectively (0,20.40,60,80,100,150,200,250,300pphr). The mechanical properties measured the device universal tensometer, such as tensile strength, elongation and modulus of elasticity, according standard specified of (ASTM D-412) were followed and the hardness property measured by (Hardness Shore A) was put through its steps according to the standard specification (ASTMD-1415). The results were selected, and the sample (10) consisting of (SIR 80/PU20 and micro-lead 300pphr) was chosen because it is more suitable for the required mechanical properties. The results observed that the ratios of micro-lead loading increased, the tensile and elongation decreased, and the hardness and elastic modulus increased. Rubber batches reinforced with micro-lead were exposed to an infrared (FTIR) test device with the addition of hexane, where there were no changes in the infrared spectrum of the rubber composites (SIR80/PU20/Micro-Pb). Sample No. (10) was shown that the scanning electron microscope (SEM) before and after adding hexane, where it was noted that the image (A) without hexane, the absence of homogeneity of lead. As for image (B) in the presence of hexane, we note the homogeneity of lead and the distribution of lead equally, so that radiation examination were measured the Geiger counter of two sources of radioactive elements were used, the caesium source $Cs^{137}$ and the cobalt source $Co^{60}$. The radiation is attenuated through the material, while the thickness of the half ($X_{1/2}$) gradually contrasts according to the attenuation of the radiation. This work is applied in the applications of shields as a protective suit against harmful radiation.

(Received December 11, 2022; Accepted March 15, 2023)

*Keywords:* Mechanical characterization, Rubber blend, Micro lead, FTIR, SEM, Shielding application

## 1. Introduction

The growing use of rubber in engineering applications results from its unique properties, including high extensibility, high strength, high energy absorption, and high fatigue resistance. Other attributes are good environmental resistance and increased resilience. Hence, the ability of rubber to undergo very high strains without permanent deformation makes it ideal for many applications. Over the past several decades, polymer blends have been one of the core areas of polymer science and technology. Polymer blends provide versatile industrial applications by enhancing properties and economic benefits. Two or more polymers have been blended for many years of similar or dissimilar nature [1,2]. A valuable technique for preparing and developing materials is the blending of two or more types of polymer with properties that exceed those of the individual components. Especially from an industrial point of view, control of the mixing state of polymer mixtures [3]. Polymer blending is one of the most critical areas in research and development due to the provision of polymer blends, a fast and cheap way to obtain new polymeric materials that appear, in general, a range of features which depend upon the properties

* Corresponding email author: mousahawannaeem@gmail.com

https://doi.org/10.15251/JOBM.2023.151.43

of their components [2]. The types of rubber and its performance have been studied earlier; it was demonstrated that the physical and mechanical properties of such blends could be significantly improved by adding a suitable compatibilist [4].

Lead is one of the most widespread heavy metals in the environment. It is a toxic substance that has received significant attention for its harmful effect on living organisms, dating back to at least 8000 years. The oldest indications of lead are in Egyptian hieroglyphics around 1500 BC in panels and statues in temples. The toxic effects were known more than 2000 years ago. Lead spreads in the earth's crust in the form of mineral ores, as these raw materials are considered natural sources that pollute the environment, and it is one of the natural elements [5]. Lead is used in manufacturing some materials, including batteries, especially car batteries, and in manufacturing water pipes and plumbing, welding cans and wire poles, and electronics. It is also used in the manufacture of ceramic and pottery utensils that may contain a dangerous amount of lead, as lead residues are a source of lead pollution [6].

Lead is a highly toxic metal (whether inhaled or ingested), affecting nearly all human body systems and organs [7]. A composite material is a material system composed of a mixture or combination of two or more macro constituents differing in form material composition and that are essentially insoluble in each other [8]. The two constituents are usually reinforcements (fibres, particulates, whiskers, laminate, flakes, or fillers). The term "reinforcement" refers to an improvement in the end–use performance of the rubber compound associated with an increase in modulus and the so-called ultimate properties, including tensile strength, tear resistance and abrasion resistance. A reinforcement filler is a particulate material that can increase: (1) the tensile strength, (2) the tear strength, and (3) the abrasion resistance of rubber. A semi–reinforcing filler is a particulate material that can increase: (1) the tensile strength; and (2) the tear strength but does not improve abrasion resistance. A non-reinforcing filler is unable to provide any increase in these properties and functions [9].

Shielding is one of the most critical factors adopted in the principles of radiation protection to reduce the risks of radiation exposure for workers in the radiation field. These shields are divided into two parts:

1. Single layer shields, which in turn are divided into two parts:

A. Pure single shields.

B. A homogeneous mixture.

2. Multi-layered shields.

The materials used to manufacture the barrier (shield) are selected according to the type of radiation to be seized and the energy of that radiation. [10].

At present, lead is used in the manufacture of protective shields from X-rays and gamma rays, there are multiple materials used as shields from radiation, and as a result of scientific development, scientists have tended to find materials with high absorption efficiency made of polymeric materials [11].

## 2. Mechanical properties

### 2.1. Hardness

Hardness is defined as the resistance of the surface of the material to scratching, furrowing, or penetration as a result of the pressure applied to the surface of the sample. Where we used Shore Hardness. According to American Standard Specifications (Durometer ASTMD-2240), the hardness is measured by pressing the indentation on the sample and reading the scale, which is listed in specific units and ranges from 0 (soft) to 100 (hard). This test may be the one that is used the most frequently in the rubber industry [12]. The International Rubber Hardness Degree IRHD, there are two types of measurement systems for hardness, which are:

The hardness measuring system (Shore) and divided into two types:

a- Hardness measurement system (Shore A) is used for soft rubber, and its range is (0-100).

b- Hardness measurement system (Shore D) is used for polymeric materials, including hard rubber, and its range is higher than (100).

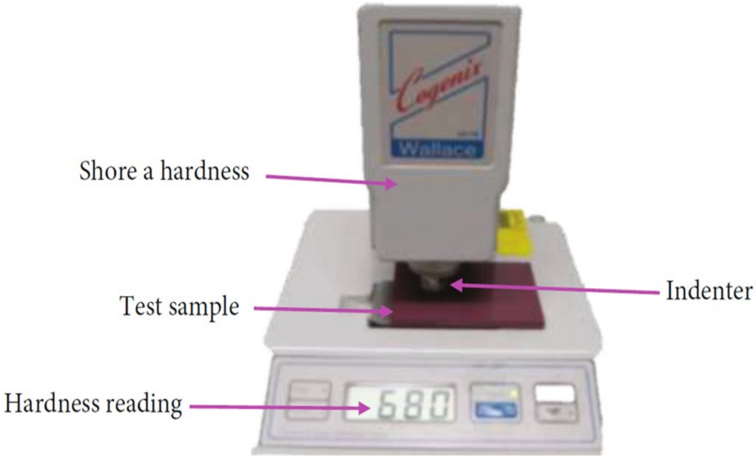


*Fig. 1. Displays the depth to which the hardness instruments have cut into, or furrowed, the rubber surface by (Shore A) [13].*

**2.2. Tensile, Elongation and Modulus**

The tensile test consists of stretching rubber samples at a uniform speed in a tensile tester and recording the stress values on the samples and the resulting elongation at more or less regular time intervals. The curve drawn with the elongation on the abscissa and the stresses on the ordinate axis is called the tensile curve. The tensile stress is the ratio of the total force acting on the sample to the initial cross-section of the sample. The tensile stress at the breaking point of the rubber sample is called tensile strength. It is defined as the force per unit area of the original cross-section, which is applied when the specimen is ruptured [14].

We can calculate the tensile strength by the equation;

$$\text{Tensile Strength} = F/\,A \quad (1)$$

where F = observed force required to break the cross section area A specimen.

Young's modulus is the ratio between the applied stress and the strain resulting from it in the elastic region in the stress elongation. In the elastic deformation of solid material, the elongation relates to the stress by a quantity called elastic modulus (E), which is the straight region in the stress-elongation curve [The following expressions describe the stress and strain;

$$\text{Stress } \sigma = \text{Force or load F/ Cross sectional area A} \quad (2)$$

$$\text{Strain } \varepsilon = (L - L_0)/\, L_0 \quad (3)$$

Thus, Young's modulus in a tensile test is given by;

$$E = \Delta\sigma\, /\Delta\varepsilon \quad (4)$$

The maximum elongation is called “elongation at break” or “ultimate elongation” Therefore; the mathematically relation to calculate the ultimate elongation is;

$$\text{Ultimate elongation} = [\, L - L_0/\, L_0] \times 100\% \quad (5)$$

where $L_0$=initial length and L=final length.

## 3. Experimental part

**3.1. The materials, which were used in this research, are:**
-Silicon Rubber (SIR) (A) and Hardener (B). Made in China.
-Polyurethane (Pu) (A) and Hardener (B). Made in China.
- Micro Lead**.** Made in India, particle size (250µm).
- Hexane. Made in India.

**3.2. Equipment**

***3.2.1. Sensitive electronic scale***

It is a device used in laboratories to determine the required quantities' weight. When used in the laboratory, it is considered clean inside and out. It is also preferable to use the same scale for the length of the experiment preparation period to avoid error, as it can determine weights with high accuracy [15].

***3.2.2. Monsanto T10 Tensometer***

The Monsanto T10 tensometer is used to carry out a number of tests, such as the Tensile Strength at Break (MPa) test, the modulus of elasticity when the elongation is (100%, 200%, 300%), (Mod300, Mod200, Mod100 MPa), and the elongation test at The cut (Elongation at Break, according to ASTM D-412-88) [16]. Where the dimensions of the sample (thickness and width) are taken this apparatus is operated by a microprocessor with a plotter and a pneumatic system to stabilize the sample before the tension test device.

***3.2.3 Hardness test device***

The device (Hardness Shore A) is used to check the hard. It is a spring-loaded device that presses against the surface of the model. The tension resulting from the spring determines the hardness of the rubber. The examination is carried out according to ASTMD-1415 and according to the Brunel method)) The model with a thickness of 4 mm is used, where the examination is performed manually. Using the device lever, the model is placed under the device, and then the device indicator begins to indicate the appropriate reading for the device (Shore A), after which the examination process is repeated four times for different areas of the model’s surface, and the average is taken [17,18].

## 4. Preparation of recipes

The components of all batches were presented in table (1), represented by fixed weight ratios of silicone rubber with fixed percentages of polyurethane with different weight percentages of micro-lead, and table (2) represents the results of the mechanical properties examination represented by hardness, tensile, elongation and modulus of elasticity.

*Table 1. The loading ratios of micro lead in (SIR-PU/Pb) composites.*

| Sample No | SIR 80 (pphr) +PU20 (pphr) | (Micro-Pb) (PPhr) |
|---|---|---|
| Sam1 | 100 | 0 |
| Sam2 | 100 | 20 |
| Sam3 | 100 | 40 |
| Sam4 | 100 | 60 |
| Sam5 | 100 | 80 |
| Sam6 | 100 | 100 |
| Sam7 | 100 | 150 |
| Sam8 | 100 | 200 |
| Sam9 | 100 | 250 |
| Sam10 | 100 | 300 |

*Table 2. Represents the mechanical properties such as hardness, tensile, elongation, strength and modulus of elasticity for different rubber composites.*

| Sample No | Hardness (Mpa) | Tensile strength (Mpa) | Elongation At % | Elastic Modulus (Mpa) |
|---|---|---|---|---|
| Sam1 | 13.8 | 0.55 | 367.5 | $1.4\times10^{-3}$ |
| Sam2 | 12.9 | 0.572 | 260.0 | $2.2\times10^{-3}$ |
| Sam3 | 15.8 | 0.946 | 340.5 | $2.7\times10^{-3}$ |
| Sam4 | 23.4 | 0.664 | 190.0 | $3.4\times10^{-3}$ |
| Sam5 | 22.5 | 0.375 | 364.5 | $1.0\times10^{-3}$ |
| Sam6 | 23.7 | 0.654 | 277.0 | $2.3\times10^{-3}$ |
| Sam7 | 24.3 | 0.475 | 158.0 | $3.0\times10^{-3}$ |
| Sam8 | 23.6 | 1.040 | 215.5 | $4.8\times10^{-3}$ |
| Sam9 | 24.8 | 0.933 | 187.0 | $4.9\times10^{-3}$ |
| Sam10 | 29.7 | 0.544 | 127.5 | $4.2\times10^{-3}$ |

## 5. Results and discussion

### 5.1. FTIR analysis

The Fourier transform-infrared (FT-IR) spectra of the rubber compound (SIR80/PU20/Micro-Pb300) and hexane were recorded at room temperature in the region (600-4000cm$^{-1}$) as shown in the above figure, where it was observed that there are no apparent changes in the radiation spectrum. Infrared for the rubber compound, even when the loading ratios changed, but the presence of hexane closed the gaps in the rubber compound, and the distribution of lead was evenly distributed. The spectra displayed the distinctive bonds of vibrations. It extends from the functional groups that were formed in the compounds from these spectra of the symmetric ($CH_3$) and asymmetric ($CH_2$) extension bands at the two regions (2848-2963cm$^{-1}$), while the ($CH_3$) band extends to the region (1452cm$^{-1}$) to the asymmetric bending vibration. The two peaks at the two areas (698-1009cm-1) are the bending vibration [19].

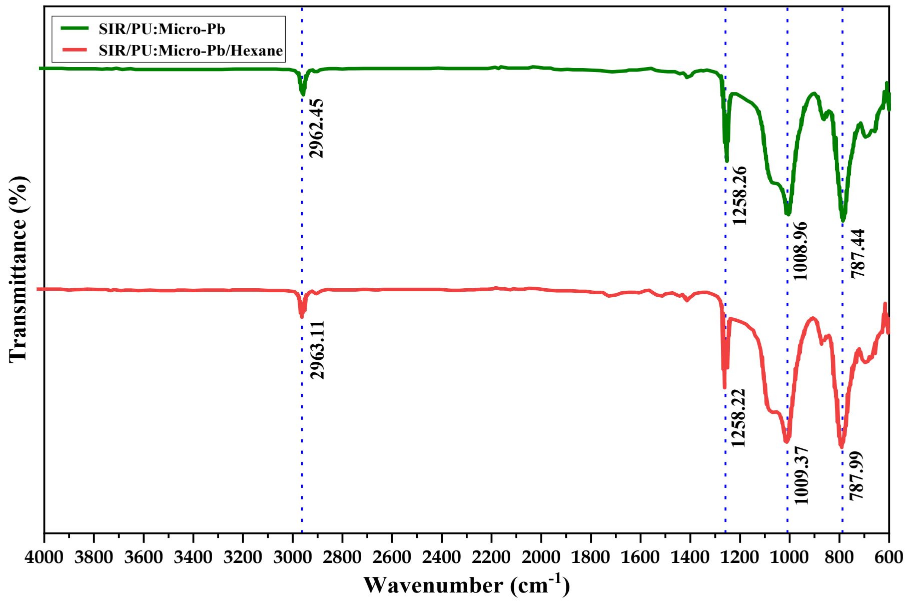


*Fig. 2. Represents rubber composite (SIR80/PU20/Micro-Pb300) of the sample without hexane and within hexane.*

### 5.2. SEM study

Sample No. (10) was shown on a scanning electron microscope before mixing hexane, representing an image (A) with lumps and heterogeneity, the micro-lead is undistributed, and there are gaps.

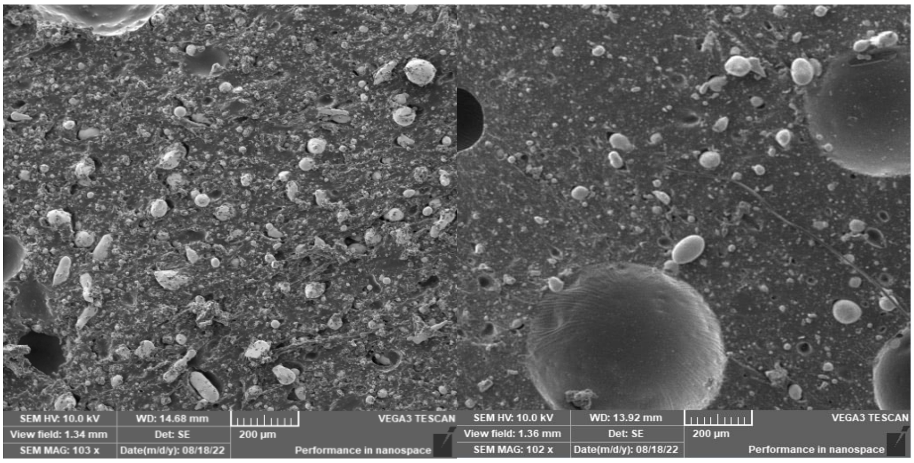


*(a)* *(b)*

*Fig. 3. Represents the image (A) of the sample without hexane and the image (B) with hexane.*

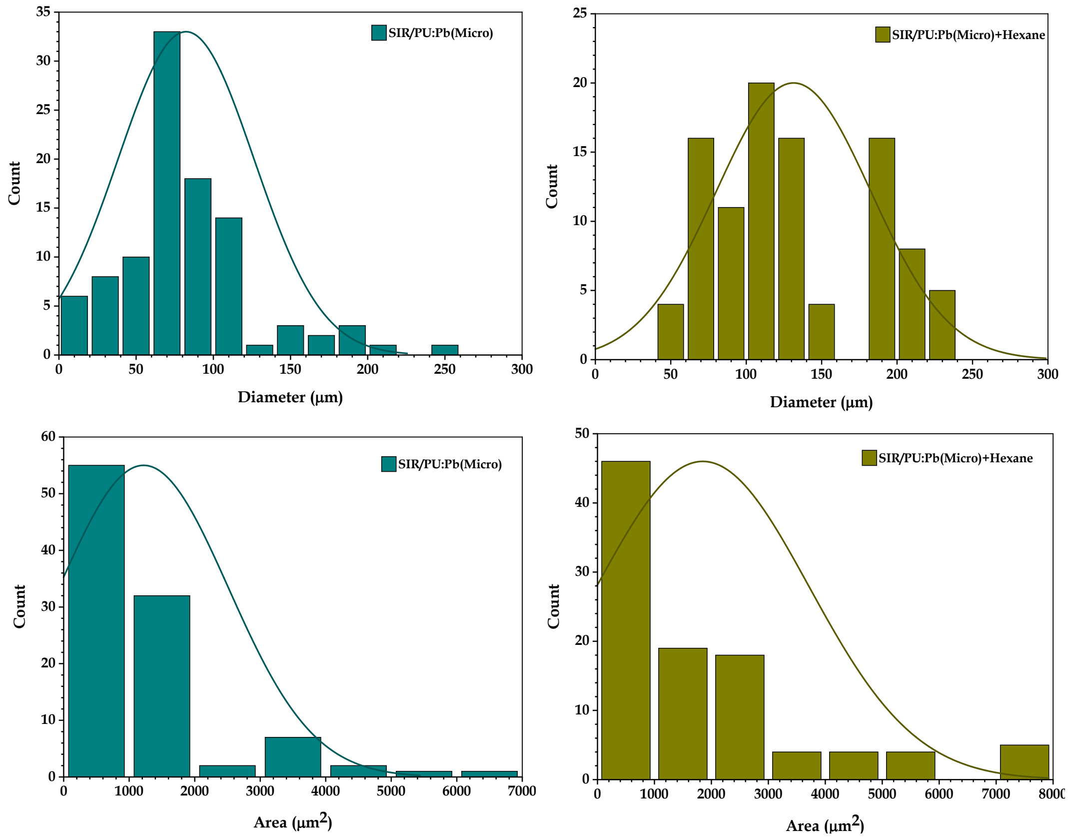


*Fig. 4. Represents the distributive function (A, $A_1$) represent the diameter and volume area of micro-lead without adding hexane. (B, $B_1$) represents the diameter and volume area of micro-lead when hexane is added.*

As for image (B), after mixing the hexane, we notice clearly that the micro-lead is distributed evenly and has no lumps; the two images are similar and have the same ingredients and quantities [20,21]. Fig. (3) represents image (A) of the sample without hexane and image (B) when hexane is added, and Fig. (4) represents the distributive function the figures (A, A1), the diameter and the volume area of the micro-lead without adding hexane, while the fig (B, B1) represents the diameter and the area of the volume of the micro-lead when adding hexane and this indicates that the micro-lead is distributed evenly on the sample, which led to the interlocking of the polymeric chains.

### 5.3. Hardness

Figure (5), it is clear that the measured hardness values for the surface of the rubber doughs increased gradually and irregularly with the increase in the amount of the additive (Micro-Pb). The reason for this is due to the interference that occurs between the supporting material and the base material, which increases the value of the hardness. The reason for this is due to the occurrence of some cross-linking between the rubber chains and the additive inside the prepared dough that is responsible for resisting the external forces applied to it, which increases the hardness of the surface of the prepared material and this agrees with previous research [22].

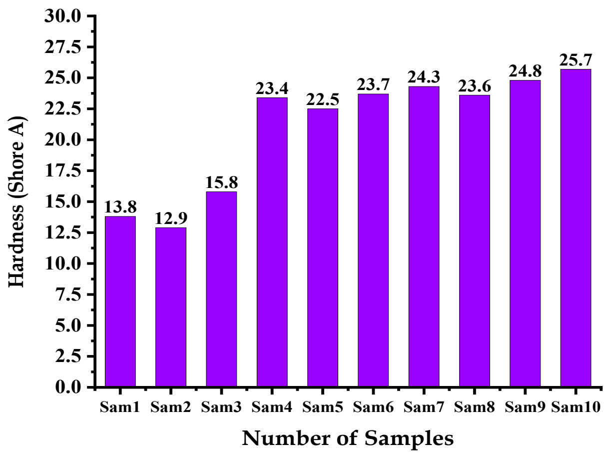


*Fig. 5. Represents change the hardness for different Rubber composite (SIR-PU/Pb).*

**5.4. Tensile Strength and elastic modulus and elongation;**

Figures (6), (7) and (8) show the effect of micro-lead powder additive with loading ratios (0,20,40,60,80,100,150,200,250,300pphr) on some mechanical properties such as tensile, modulus of elasticity and elongation of the rubber compound consisting of silicone rubber (80). and polyurethane (20) for rubber batches, and as a result of the comparison between the effects of mechanical tests (tensile resistance, modulus of elasticity and elongation) as well as the radiation properties of the dough models, the sample (10) with components (SIR80/PU20 /Pb-micro) was more appropriate. It achieved the mechanical properties as We notice from the figures a slight increase in the tensile strength, modulus of elasticity and a decrease in the amount of elongation with the increase in the loading ratio of the micro-lead powder. This is due to the rise in the physical bonding and the cohesion of the filler with rubber. The micro-lead powder (Pb-micro) has a small granular size that increases the surface area for diffusion and, thus, the formation of a larger amount of crosslinking with the rubber chains, and this is consistent with previous research [22]. It is also noted from the figures that the decline in the tensile and elongation resistance scheme is explained based on the material reaching the point of submission, where the material continues to resist until its resistance collapses as a result of the lack of distance between the rubber chains, as they are at a certain percentage that cannot withstand the added substance, which leads to cracks and poisons in the sample Elasticity and this is consistent with previous research [23]. As for the increase in the modulus of elasticity, it can indicate a strong drop in elongation, and as a result of its inverse proportion to the modulus of elasticity property, the cause of a clear increase in the modulus of elasticity and this resulted in a slight decrease in the tensile strength property.

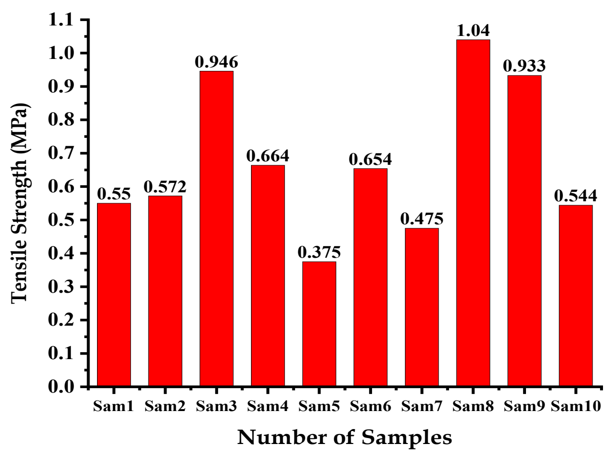


*Fig. 6. Represents change the tensile strength for different Rubber composite (SIR-PU/Pb).*

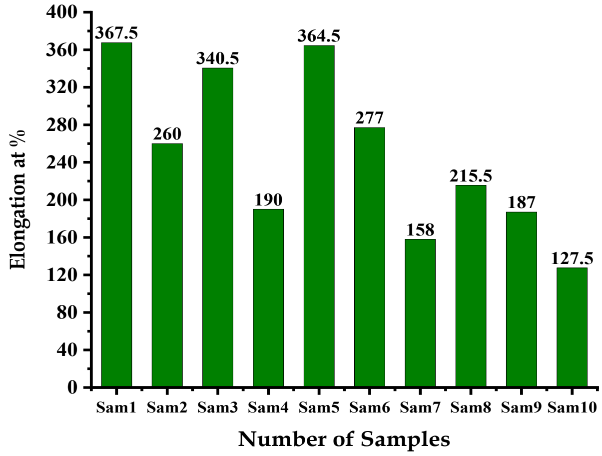


*Fig. 7. Represents change the elongation for different Rubber composite (SIR-PU/Pb).*

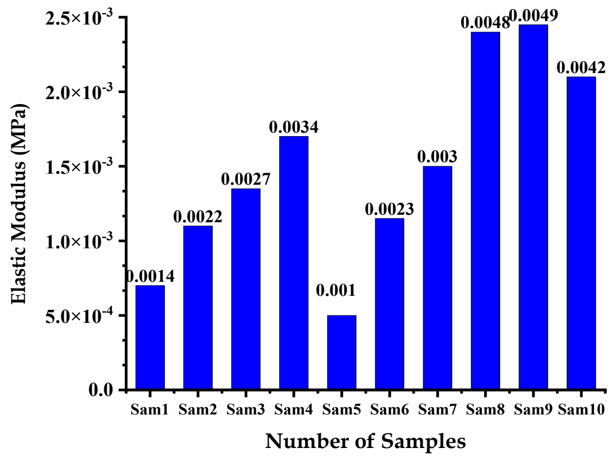


*Fig. 8. Represents change the elastic modulus for different Rubber composite (SIR-PU/Pb).*

## 6. Results of radiation examinations

### 6.1. Calculation of the thickness of the half $X_{1/2}$, the linear absorption coefficient μ, and the mass absorption coefficient $\mu_m$ when using the cesium source $Cs^{137}$

The values of the half-thickness are practically determined through Figure (9), which shows the graphical relationship between thickness and penetrating radiation (N) when using the $Cs^{137}$ radiating source and for different loading ratios of (Pb-micro). Where it was noticed a decrease in the value of the thickness of the half $X_{1/2}$ and an increase in both the linear and mass absorption coefficients with the increase in the loading ratios. This is due to the efficiency of the prepared compound in absorbing and attenuating the used rays, and this efficiency increases with the increase in the percentage of loading of the microscopic lead powder [24,25], see the table (3).

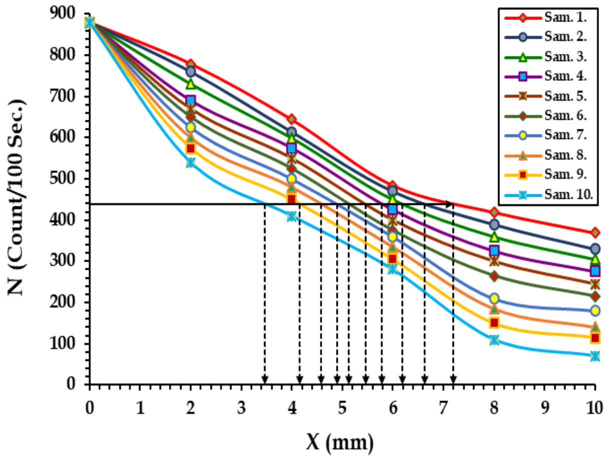


*Fig. 9. The graphical relationship between thickness and the number of penetrating radiation (N) when using a source (cesium $Cs^{137}$) for different loading ratios of (Pb-micro).*

*Table 3. Linear and mass absorption coefficient and half thickness of cesium source $Cs^{137}$ for different loading ratios of Pb-micro powder for rubber samples.*

| Batch No | Lead PPhr | $X_{1/2}$ (mm) | μ ($cm^{-1}$) | $\mu_m$ ($cm^2$/gm) |
|---|---|---|---|---|
| A | 0 | 7.192 | 0.964 | 2.814 |
| B | 20 | 6.634 | 1.045 | 1.051 |
| C | 40 | 6.193 | 1.119 | 0.379 |
| D | 60 | 5.786 | 1.198 | 0.992 |
| E | 80 | 5.463 | 1.269 | 1.035 |
| F | 100 | 5.127 | 1.352 | 0.872 |
| G | 150 | 4.896 | 1.416 | 0.794 |
| H | 200 | 4.583 | 1.512 | 0.753 |
| I | 250 | 4.162 | 1.665 | 0.689 |
| J | 300 | 3.472 | 1.996 | 0.719 |

### 6.2. Calculation of the thickness of the half $X_{1/2}$, the linear absorption coefficient μ, and the mass absorption coefficient $\mu_m$ when using the cesium source $Co^{60}$:

The second source of electromagnetic radiation was used, the $Co^{60}$ source, where the overlaid rubber models were examined. We noticed a decrease in the thickness of the half when the ratio of loading the additive was increased. Mainly on the number of particles present in the path of radiation, Fig (10) and Table (4) show the results obtained for cobalt source $Co^{60}$ [26,27].

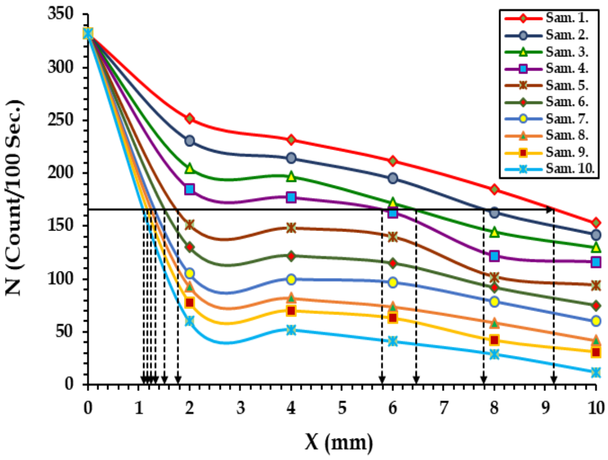


*Fig. 10. The graphical relationship between thickness and the number of penetrating radiation (N) when using a source (cesium $Co^{60}$) for different loading ratios of (pb-micro).*

*Table 4. Linear and mass absorption coefficient and half thickness of cesium source $Co^{60}$ for different loading ratios of pb-micro powder for rubber samples.*

| Batch No | Lead PPhr | $X_{1/2}$ (mm) | $\mu$ ($cm^{-1}$) | $\mu_m$ ($cm^2/gm$) |
|---|---|---|---|---|
| A | 0 | 9.177 | 0.755 | 2.205 |
| B | 20 | 7.782 | 0.891 | 0.896 |
| C | 40 | 6.459 | 1.073 | 0.364 |
| D | 60 | 5.792 | 1.197 | 0.991 |
| E | 80 | 1.781 | 3.893 | 3.174 |
| F | 100 | 1.510 | 4.591 | 2.960 |
| G | 150 | 1.327 | 5.225 | 2.932 |
| H | 200 | 1.249 | 5.548 | 2.764 |
| I | 250 | 1.172 | 5.912 | 2.447 |
| J | 300 | 1.101 | 6.296 | 2.267 |

## 7. Conclusions

In this study, the results showed a significant improvement in the structural and mechanical properties after adding lead microparticles to the rubber compound in different ratios, as the structural properties of FT-IR did not show any significant chemical interaction. In contrast, the SEM measurements showed a homogeneous distribution with increasing lead concentration. While the mechanical properties of hardness, tensile strength, elongation, and modulus of elasticity improved significantly, this makes the microcomposites more suitable to be applied to radiation shielding, as radiation attenuation was shown on a sample (10) with microcomposites of (SiR80/PU20/micro-Pb300 pphr), which leads to good results, especially in $Co^{60}$ attenuation.

## Acknowledgements

The authors gratefully acknowledge the department of physics, the University of Babylon, Iraq for their support.

## References

[1] Kumagai, S., & Yoshimura, N. (2001), IEEE Transactions on dielectrics and electrical insulation, 8(2), 203-211; https://doi.org/10.1109/94.919930.
[2] Slutzky, G. M., & Ji, T. H. (1974), Biochimica et Biophysica Acta (BBA)-Biomembranes, 373(3), 337-346; https://doi.org/10.1016/0005-2736(74)90013-3.
[3] Findik F.,Yilmas R.,Kokas T., Materials and design J.Vol.25,pp 269-276, 2004; https://doi.org/10.1016/j.matdes.2003.11.003.
[4] Levin, M. (2007), The Journal of philosophy, 104(9), 433-463 ; https://doi.org/10.5840/jphil200710498.
[5] Cormont, A., Siepel, H., Clement, J., Melman, T. C., WallisDeVries, M. F., van Turnhout, C. A. M., ... & De Snoo, G. R. (2016), Journal for Nature Conservation, 30, 19-26; https://doi.org/10.1016/j.jnc.2015.12.006.
[6] Lanphear, B,P;Hornung, R;and Khoury,J (2005), Environ health Perspect.113(7):894-899; https://doi.org/10.1289/ehp.7688.
[7] Fankina, I. V., Furtsev, A. I., Rudoy, E. M., & Sazhenkov, S. A. (2022), Philosophical Transactions of the Royal Society A 380(2236), 20210354; https://doi.org/10.1098/rsta.2021.0354.
[8] Alsaman, A. S., Ibrahim, E. M. M., Askalany, A. A., Farid, A. M., Ali, E. S., & Ahmed, M. S. (2022), Chemical Engineering Research and Design, 188, 417-432; https://doi.org/10.1016/j.cherd.2022.09.017.

[9] Ishiaku, U. S., Pang, K. W., Lee, W. S., & Ishak, Z. M. (2002), European Polymer Journal, 38(2), 393-401; https://doi.org/10.1016/S0014-3057(01)00125-2
[10] Claessens, M., Oria, C. S., Brouwer, C. L., Ziemer, B. P., Scholey, J. E., Lin, H., ... & Verellen, D. (2022, October), In Seminars in Radiation Oncology (Vol. 32, No. 4, pp. 421-431). WB Saunders; https://doi.org/10.1016/j.semradonc.2022.06.011
[11] Fu, P., Li, H., Gong, J., Fan, Z., Smith, A. T., Shen, K., ... & Sun, L. (2022), Progress in Polymer Science, 101506. https://doi.org/10.1016/j.progpolymsci.2022.101506
[12] Schettgen, T., Esser, A., Kraus, T., & Ziegler, P. (2022), Chemosphere 291, 132722; https://doi.org/10.1016/j.chemosphere.2021.132722.
[13] Ud Din, S., Chaudhary, F. A., Ahmed, B., Alam, M. K., Parker, S., Patel, M., & Javed, M. Q. (2022), BioMed Research International, 2022; https://doi.org/10.1155/2022/1703869.
[14] Mustafa, B. S., Jamal, G. M., & Abdullah, O. G. (2022), Results in Physics 105662; https://doi.org/10.1016/j.rinp.2022.105662
[15] Wang, Q., Jian, M., Wang, C., & Zhang, Y. (2017), Advanced Functional Materials **27**(9), 1605657; https://doi.org/10.1002/adfm.201605657.
[16] Mansour khaki, A., Ameri, M., Habibpour, M., & Underwood, B. S. (2020), Construction and Building Materials, **239**, 117800; https://doi.org/1010.16 / j.conbuildmat.2019.117800.
[17] Al-Nesrawy, E. F., & Al-Nesrawy, S. H. H. (2021, August), Journal of Physics: Conference Series **1973**, No. 1, p. 012161, IOP Publishing; https://doi.org/10.1088/1742-6596/1973/1/012161.
[18] Naeem, M. H., & Al-Nesrawy, S. H. H. (2019), Preparation of (Rubber Blend/Oyster Shell Powder) Composites and Study Rheological Properties; https://doi.org/10.36478/jeasci.2019.10092.10097.
[19] Meteab, M. H., Hashim, A., & Rabee, B. H. (2022), Silicon, 1-12; https://doi.org/10.1007/s12633-022-02114-7
[20] Meteab, M. H., Hashim, A., & Rabee, B. H. (2022), Silicon, 1-11; https://doi.org/10.1007/s12633-022-02020-y.
[21] Khorasani, M. T., MoemenBellah, S., Mirzadeh, H., & Sadatnia, B. (2006), Colloids and Surfaces B: Biointerfaces, **51**(2), 112-119; https://doi.org/10.1016/j.colsurfb.2006.06.002.
[22] Mostafa, A., Abouel-Kasem, A., Bayoumi, M. R., & El-Sebaie, M. G. (2009), *Materials & Design*, **30**(5), 1561-1568; https://doi.org/10.1016/j.matdes.2008.07.043.
[23] Mittelman, A., & Roman, I. (1990), Composites, **21**(1), 63-69; https://doi.org/10.1016/0010-4361(90)90099-I.
[24] Han, I., Aygun, M., Demir, L., & Narmanlı, E. (2011), *J*ournal of X-Ray Science and Technology **19**(4), 501-508; https://doi.org/10.3233 / XST-2011-0309.
[25] Mahmoud, I. S., Issa, S. A., Zakaly, H. M., Saudi, H. A., Ali, A. S., Saddeek, Y. B., ... & Tekin, H. O. (2021), Journal of Alloys and Compounds **888**, 161419; https://doi.org/10.1016/j.jallcom.2021.161419
[26] Reda, S. M., & Saleh, H. M. (2021), Progress in Nuclear Energy, **142**, 104012; https://doi.org/10.1016/j.pnucene.2021.104012
[27] Buyuk, B., & Tugrul, A. B. (2014), Annals of Nuclear Energy **71**, 46-51; https://doi.org/10.1016/j.anucene.2014.03.026.